AD-A045 867 MARYLAND UNIV COLLEGE PARK COMPUTER SCIENCE CENTER F/G 14/5
A SURVEY OF RANDOM PATTERN GENERATION PROCESSES.(U)
JUL 77 B SCHACHTER, N AHUJA AFOSR-77-3271
UNCLASSIFIED CSC-TR-549 AFOSR-TR-77-1225 NL

1 OF 1
AD
A045867

END
DATE
FILMED
11-77
DDC

AFOSR-TR- 77 - 1225

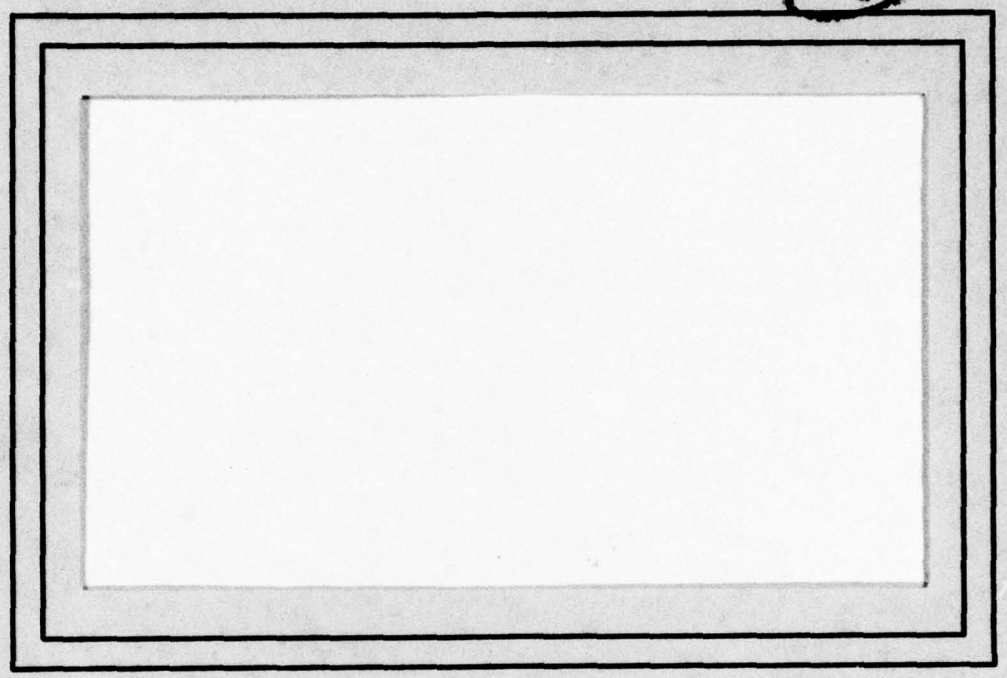

COMPUTER SCIENCE TECHNICAL REPORT SERIES

UNIVERSITY OF MARYLAND
COLLEGE PARK, MARYLAND
20742

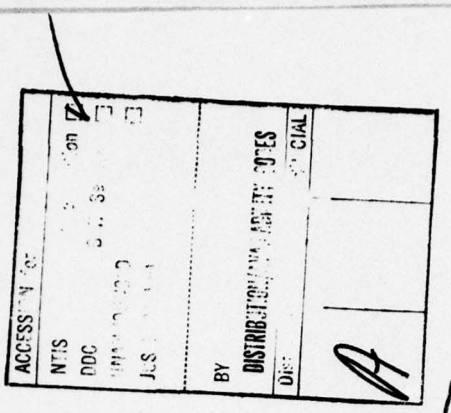

(12)

(14) CSC - TR-549

(15) AFOSR-77-3271

(11) July 1977

(12) 42p.

(6)

A SURVEY OF RANDOM PATTERN GENERATION PROCESSES.

(10) Bruce/Schachter
Narendra/Ahuja
Computer Science Center
University of Maryland
College Park, MD 20742

(16) 2304 (17) A2 (18) AFOSR

(9) Technical rept.

ABSTRACT (19) TR-77-1225

Random pattern generation processes can provide a rich class of models for both the synthesis and analysis of visual textures. This report describes a variety of such processes including point processes, random mosaic processes, and bombing processes. Standard texture analysis approaches (e.g., cooccurrence matrices) are related to texture models based on these random processes. Examples of several textures synthesized by computer in accordance with these models are presented.

The support of the Directorate of Mathematical and Information Sciences, U.S . Air Force Office of Scientific Research, under Grant AFOSR-77-3271, is gratefully acknowledged, as is the help of Mrs. Shelly Rowe in preparing this paper.

403 018

1. Introduction

Random two-dimensional vector patterns are commonly encountered in geology, metallurgy, oceanography, and in all types of photographic image processing. For convenience, we will refer to all such random vector fields as multicolor patterns, even when the vectors of the process describe features other than color.

We are interested in how patterns are formed and what parameters are needed to describe them. We will ask the following questions: What are the proportions of the various colors? When we move around the pattern, what are the probabilities of the transitions from one color to the next? What shapes are the pieces that comprise the pattern, and how are these pieces combined? We would like to know the first and second order statistics of our patterns, e.g., histograms, variograms; and the coocurrences and differences of colors at the endpoints of a dropped Buffon needle.

One of the principal applications of the study of random patterns is to the analysis and synthesis of visual textures. First and second order statistics are commonly used as features for texture classification. If textures can be modeled as random patterns, it should be possible to predict the effectiveness of such features and to design optimal features for various tasks.

The purpose of this report is to present information about a variety of spatial pattern models, including point processes, random mosaics, and bombing models. We describe a

number of models for spatial point patterns in Section 2. The "most random" of these, the Poisson point process, will be used in the construction of most of the succeeding patterns.

In Section 3, we will model piecewise contiguous patterns by random mosaics. One of these models, the Poisson Line model, has interesting Markovian properties. Another, the Occupancy model, mimics natural cell growth processes. The use of mosaics to depict patterns is of course ancient. The Chaldeans were skilled mosaicists by 2500 BCE. The Greeks further developed the art and were thought to have used pattern books for standard motifs. The pieces of a mosaic were known to the Romans as tesserae or tessellae. A mosaic having a simple geometric design was known as opus tesselatum -- giving rise to the current term "tessellation".

We will discuss bombing models in Section 4. The bombs are geometric figures that are dropped onto a plane. These figures in union are the foreground of a pattern, with the uncovered portion of the plane forming the background. Many natural two-color patterns are formed by bombing processes or at least can be modelled by them; e.g., bubble holes on the surface of cement, leaves on the ground, pebbles on a beach, small stones on the surface of asphalt, etc.

Some statistical properties of our models will be noted in Section 5. Finally, in Section 6, we will suggest projects for future research.

Realizations of all the primary models covered in Sections 2 through 4 will be generated on the computer.

2. Point Processes

A two-dimensional Poisson process, with intensity λ, can be used to describe a random distribution of points on the plane. (The parameter λ is called the intensity or density of the process.) This process is characterized by the property that the expected number of points in a region of area A is λA, irrespective of the orientation or shape of the region.

A two-dimensional Poisson point process can be easily simulated on the computer. A random number generator is used to generate λ pairs (x_o, y_o), where (x_o, y_o) are the coordinates of a point in the unit square (Fig. 1). These points can be thought of as dropped onto the square, like raindrops falling on a puddle, or meteorites striking the moon.

Not all point distributions are random; a point's nearest neighbors, e.g., may be closer or farther than predicted under a Poisson model. Examples of such processes [1] are briefly discussed below, but will not be used to generate any of the textures discussed in this paper.

1a) Contagious model: Particles are attracted to their neighbors. An example of such a process is the spatial distribution of social animals.

1b) Clustering model (center-satellite process): Particles are parents (or nuclei) of families of children (satellites). The parents may be dispersed in a Poisson manner with their children congregating about them. A good example of such a process is bushes in a field that reproduce by sending off shoots.

1c) Doubly stochastic Poisson model [2]; Heterogeneity is introduced by allowing the density of points to be a function of location; i.e., $\lambda = \lambda(x,y)$. For instance, λ might be dependent on local fertility or microclimate.

2) Inhibitory model: Particles repel their neighbors, as if they were animals defending their territory.

The distribution of a space-time point process may be a function of a time varying intensity λ. Consider a forest that starts with a random scattering of trees. As the forest gets denser, the trees crowd each other out, since they cannot occupy the same space at the same time. Thus constraints are imposed upon the location of newly introduced points. The distribution of trees changes with time from a Poisson to an inhibitory process.

3. Cell Structure Models

Many natural scenes are composed of regions that appear textured; the regions themselves are often composed of relatively distinct patches of different colors. For instance, when we view a terrestrial landscape from the air we see a mosaic of different plant species and land uses. Expensive agricultural machinery fosters the regionalization of crops into large fields. Urban, suburban, desert, mountainous, and water regions all have distinct appearances from the air. Such regions can be modelled by random mosaics [3]. In this section we will describe a family of pattern generation processes that can produce random mosaics.

Random mosaics are constructed in two steps:

1) Tessellate a planar region into cells. We will only consider tessellations composed of bounded convex polygons.

2) Independently assign one of m colors to each cell according to a fixed set of probabilities

$$p_1,\ldots,p_m;\ \sum_{i=1}^{m} p_i = 1.*$$

---

*Other random coloring schemes are possible. Examples: (i) Each cell has a constant color throughout, where the constants are independently chosen from a single normal distribution. (ii) All cell borders are given a thickness and one color, and all cell interiors are given a second color.

By this process, we partition region A into subregions $A_1,\ldots,A_m$; $\bigcup_{j=1}^{m} A_j = A$, where A_j is defined to be the union of all cells of color j. The partitioning of A is the realization of a random process with the following stationary and transition probabilities:

(1) For all $s\in A$, $\Pr(s\in A_i) = p_i$ for $i = 1,2,\ldots,m$.

(2) For all $(s,s')\in A$, with distance $d = |s-s'|$ between them, $\Pr(s'\in A_i | s\in A_j) = P_{ij}(d) = p_i(1-W(d)) + \delta_{ij}W(d)$ for $i,j=1,2,\ldots,m$. $W(d)$ is the probability that any two points that are distance d apart are both in the same cell, and δ_{ij} is the Kronecker delta.

Cell structure models form a family whose members differ only in the manner in which the plane is tessellated. We will describe some important members of this family, starting with the most random members and progressing toward more regular examples.

The first model we will consider is a Gaussian random process. It is a degenerate form of a cell structure model, in that each point of an image constitutes an entire cell.

Nondegenerate cell structure models are constructed by two types of processes: (1) line processes and (2) cell growth processes. The first type of process uses straight lines to partition a region into cells. The positions and orientations of these lines can range from randomly distributed (Poisson line model) to regularly arranged (Checkerboard model). The second type of process uses a spatial

point process to generate the nuclei of growing cells. If the nuclei are randomly positioned an Occupancy model is produced.

3.1 Gaussian Random Process

A real random vector process $\{Y_{s_i} \mid s_i \in A\}$ is a Gaussian random process if for every finite set of points $\{s_i\} \in A$, the corresponding random vectors Y_{s_i} are jointly Gaussian random vectors. A (stationary) Gaussian random vector process is completely defined (statistically) by its mean $\mu = E(Y_{s_i})$ and auto-covariance matrix $\Sigma(b)$, where $\Sigma(b) = E[(Y_{s_{i+b}} - \mu)(Y_{s_i} - \mu)^t]$. The process reduces to one of white noise if $\Sigma(b) = \Sigma(0) \cdot \Delta(b)$, where $\Delta(b) = 1$ when $b = 0$, and $\Delta(b) = 0$ otherwise.

3.2 Random Line and Cell Growth Processes

a) Poisson Line Model: $L(\frac{\tau}{\pi}, p_1, \ldots, p_{m-1}, \mu_1, \ldots, \mu_m, \Sigma_1, \ldots, \Sigma_m)$

Consider a system of intersecting lines in the plane with random positions and orientations. Such a system when derived by the following Poisson process possesses fundamental properties of homogeneity and isotropy. A Poisson process of intensity τ/π chooses points (θ,p) in the infinite rectangular strip $[0 \leq \theta < \pi, -\infty < p < \infty]$. Each of these points can be used to construct a line in the plane of the form $x\cos\theta + y\sin\theta - p = 0$, where p is the distance to an arbitrarily chosen origin. One can use this process to tessellate any finite region A into cells (Fig. 2a). It can be seen that there are almost certainly four cells converging at each vertex. These cells are then colored in the manner previously described.

The sequence of colors obtained by sampling an n-color Poisson line mosaic at equal intervals is an n-state discrete Markov chain with transition matrix P(d) given by

$$P(d) = \begin{array}{c} \\ A_1 \\ A_2 \\ \vdots \\ A_m \end{array} \begin{array}{c} \begin{array}{cccc} A_1 & A_2 & \cdots & A_m \end{array} \\ \begin{bmatrix} P_{11}(d) & P_{21}(d) & \cdots & P_{m1}(d) \\ P_{12}(d) & P_{22}(d) & \cdots & P_{m2}(d) \\ \vdots & \vdots & & \vdots \\ P_{1m}(d) & P_{2m}(d) & \cdots & P_{mm}(d) \end{bmatrix} \end{array}$$

where d is the sampling interval. A matrix of the above form is a necessary but not sufficient condition for randomness. The additional requirement for the random mingling of the color

cells places a further restriction on P(d); namely $P_{j\alpha} = P_{j\beta}$ for all $\alpha, \beta \neq j$. A Markov transition matrix having this form possesses the following properties [4, 5]:

(1) Reversibility - The probability that color region A_i follows A_j in the sampling sequence is the same as the probability that A_j follows A_i. This condition can be expressed in terms of the stationary and transition probabilities of the process:

$$p_j P_{ij}(d) = p_i P_{ji}(d), \text{ where } P_{ij}(d) = P_i(1-W(d)) + \delta_{ij} W(d)$$

$$\text{and } W(d) = e^{-2\tau d/\pi} .$$

It can be shown that this condition reduces to

$$P_{ii}(d) - P_{jj}(d) = \text{a constant} = \gamma \text{ for } 1 \leq i, j \leq n, i \neq j.$$

There are many situations when a texture does not possess this property. For example, consider an aerial photograph of a field where the distribution of plant species is controlled by the prevailing winds or predominant direction of sunlight.

(2) Lumpability - The chain resulting from any regrouping or renaming of the color states is still Markov.

(3) Specifiability - A random m-color Poisson line mosaic is completely specified by 3m parameters. To specify the area covered by each of the colors we need to provide any m-1 independent terms of the stationary probability vector $(p_1 p_2 \ldots p_m)$. To specify the transition matrix we need P_{ij} for all i and j. However the following restrictions mean that the entire matrix can be specified by only one parameter, namely the constant γ:

(i) $p_i = p_i P_{ii}(d) + P_{ij}(d) \sum_{k \neq i} p_k$; $1 \leq i, j \leq m$, $i \neq j$

(ii) $P_{ii}(d) - P_{kk}(d) =$ a constant $= \gamma$.

The constant γ is proportional to the expected cell width $E(w) = \frac{2}{\tau}$. An additional 2m parameters are needed for the means and covariances of the m colors.

(4) The chain is irreducible, aperiodic, and all its states are recurrent states, since $0 < P_{ij}(d) < 1$ for all i and j. These properties are defined as follows. The period of state α of a Markov chain is the greatest common divisor of all integers $n \geq 1$ for which the probability of returning to state α, starting from state α, in n steps is nonzero. A Markov chain is aperiodic if its period is 1. A Markov chain is irreducible if all its states are accessible from each other. A state of a Markov chain is recurrent if when we start from the state we will eventually return to it.

Two or more contiguous cells of the same color are said to form a patch. We would next like to derive the ratio of patch width to cell width. Consider the distribution of length ℓ_α of color α along a transect. It can be shown [4] that the sizes of neighboring cells are independent for a Poisson line tessellation. The points of intersection of an arbitrary line with a Poisson line tessellation constitute a Poisson line process with intensity $2\tau/\pi$. This means that the expected number k of lines crossing a transect of unit length is $2\tau/\pi$. Thus ℓ_α is the sum of j independent values of $1/k$. Let $g(\ell_\alpha | j)$ denote the conditional pdf of ℓ_α given j. Then

$$g(\ell_\alpha|j) = \frac{(\frac{2\tau}{\pi})^j \ell_\alpha^{j-1} e^{-(\frac{2\tau}{\pi})\ell_\alpha}}{(j-1)!}$$

A run of j cells of color α will occur if the succeeding j-1 cells are of color α and a cell of another color follows to terminate the run. The probability that this will happen is $p_\alpha^{j-i}(1-p_\alpha)$. The conditional pdf of ℓ_α when j is allowed to vary is therefore

$$g(\ell_\alpha) = \sum_{j=1}^{\infty} g(\ell_\alpha|j) p_\alpha^{j-1}(1-p_\alpha)$$

$$= \frac{2\tau}{\pi}(1-p_\alpha)\, e^{-\frac{2\tau}{\pi}\ell_\alpha} \sum_{j=1}^{\infty} \frac{(\frac{2\tau}{\pi} p_\alpha \ell_\alpha)^{j-1}}{(j-1)!}$$

$$= \frac{2\tau}{\pi}(1-p_\alpha)\, e^{-\frac{2\tau}{\pi}\ell_\alpha(1-p_\alpha)}$$

Thus the expected width of a patch of color α is $1/(1-p_\alpha)$ times the expected cell width.

Showing that a texture fits a Poisson line model requires the proof of a very complicated hypothesis. We must show that i) the pattern is not directionally dependent, ii) cells of all colors are randomly mingled, and iii) the pattern of each color when taken against a background of the remaining colors forms a 2-color Poisson line mosaic.

b) Occupancy Model

The occupancy model is defined as follows. A Poisson process with intensity λ drops points onto the plane. Each of these points spreads out to occupy a "Dirichlet cell"

consisting of all points on the plane that are nearer to it than to any of the other Poisson points. These cells are convex Voronoi polygons having, on average, six sides (Fig. 2d). (It can be shown [6] that nearest neighbors can be determined in $\Theta(\lambda \log \lambda)$ time.) These cells are then independently assigned colors as usual.

Two models that are related to the occupancy model will be briefly noted. A random triangular tessellation can be constructed from Delaunay triangles [8] that have as their vertices the three nuclei that are equidistant from a vertex of a Voronoi polygon. Thus the intersections of the borders of Voronoi polygons are the circumcenters of the Delaunay triangles (see Fig. 3).

The Johnson-Mehl model [7] is often used to describe metallurgical surfaces. This model differs from the occupancy model only in that points are dropped onto the plane as a function of time; i.e., $\lambda = \lambda(\tau)$. These points start expanding circularly as soon as they hit the plane. A point on the plane is assigned to the cell whose expanding border first reaches it. Cells formed by this process do not have straight line edges and are not necessarily convex (Fig. 4). Irregular configurations occur when late arriving points fall near the interface of two large cells.

The occupancy model simulates natural cell growth processes on the plane. In contrast, true Poisson line mosaics are surely rare in nature. There are, however, several good reasons for choosing the Poisson line model as a standard

with which to compare natural mosaic patterns:

(1) The Poisson line model is mathematically more tractable. We do not have an elementary form for W(d) for the occupancy model [9].

(2) The sizes of adjacent cells are independent for the Poisson line model, but not for the occupancy model [4].

(3) We would not expect cells formed by a natural process to have the sharp corners produced by a Poisson line tessellation. But a natural texture for which the variance of cell size closely resembles that of the Poisson line model is perfectly plausible [4].

3.3 Regular Line and Cell Growth Processes

a) Rotated Checkerboard Model: $C(b,p_1,\ldots,p_{m-1},\mu_1,\ldots,\mu_m,\Sigma_1,\ldots,\Sigma_m)$

This is an example of a cell structure model where the cells have a uniform diameter. A checkerboard model can be formed by the following procedure. First choose the origin of an x-y coordinate system on the plane with uniform probability density. Then tessellate the plane into square cells of side length b. Next, this "checkerboard" is rotated by an angle chosen with uniform probability from the interval $(0,2\pi)$. The cells are now independently assigned one of the m tile types as before (Fig. 2h). The solution for W(d) for this model is discussed in the statistics literature as an extension of Buffon's needle problem:

$$W(d) = 1 - 4d/\pi b + d^2/\pi b^2;\ d \le b$$

$$= 1-2/\pi - (4/\pi)\cos^{-1}(b/d) - d^2/\pi b^2 + (4/\pi)(d^2/b^2-1)^{\frac{1}{2}};\ b < d \le \sqrt{2}\, b$$

$$= 0;\ d > \sqrt{2}\, b.$$

b) Rotated Hexagon Model [10]: $H(\lambda,p_1,\ldots,p_{m-1},\mu_1,\ldots,\mu_m,\Sigma_1,\ldots,\Sigma_m)$

This model is analogous to the checkerboard model, except that hexagons are used in place of squares. Another way of viewing these models is as follows: Consider a system of particles on the vertices of a regular lattice (Figs. 5,6a). Let these particles be the nuclei of growing cells. Cells will

grow unimpeded in a circular fashion until they reach the tightly packed state shown in Figures 5,6b. At this moment each circle has four or six points of contact with its neighbors, depending on the nature of the lattice. As the cells continue to grow these points of contact will be extended into lines, and the equal circles shown in Figures 5,6b will be converted into the equal hexagons or squares shown in Figures 5,6c. Notice the duality between a hexagonal and triangular tessellation (Fig. 7).

4. Bombing Models

Random two-color patterns can be formed by bombing processes. The bombs are geometric figures that are dropped onto the plane. The sizes and shapes of these figures are fixed, but their positions and orientations are random. The location of a figure is determined by its center point (x_o, y_o) (i.e., center of gravity), and the orientation Θ of its principal axis. By this process a fixed region A is randomly partitioned into A_1 and $A_2 = A - A_1$, where A_1 consists of that part of A that is covered by the dropped figures. We shall refer to the figures comprising A_1 as isotropically distributed.

We are assuming translation invariance. Hence the number of center points falling on any subregion of the plane depends only upon the area of the subregion -- not on its shape or orientation. The number of center points falling on any subregion A has a Poisson distribution with mean λA, where λ is the expected number of center points falling on any unit area of the plane.

To complete the specification of our model, we will color regions A_1 and A_2 in a Gaussian fashion, with distributions $N(\mu_1, \Sigma_1)$ and $N(\mu_2, \Sigma_2)$ respectively. We will now consider three coverage theorems for bombing processes.

Let K be a randomly positioned convex figure with fixed orientation Θ. Let K_o be another convex region. Let $\alpha(K_o, K, \Theta)$ denote the area in which the center point of K can be placed so that K intersects K_o. The area $\alpha(K_o, K, \Theta)$ has as its border the locus of points where the center point of K might fall

so that the region K with orientation θ just touches the borders of K_o (Fig. 8).

The measure of all center points of the figure K where it intersects K_o is

$$m(K_o,K) = \int_o^{2\pi} \alpha(K_o,K,\theta)\, dF\theta$$

where $F(\theta)$ is the distribution function of the orientation parameter θ.

Theorem I (Dufour) [11]: Consider an infinite collection of congruent figures K independently, identically, and homogeneously distributed over the plane. The number of figures K intersecting another convex figure K_o has a Poisson distribution with mean $\lambda m(K_o,K)$.

Theorem II (Dufour) [11]: Consider an infinite collection of congruent random figures of area a and perimeter L distributed isotropically, independently, and homogeneously throughout the plane. The number of such figures intersecting another convex figure of area a_o and perimeter L_o has a Poisson distribution with mean $\lambda(a_o + a + L_oL/2\pi)$.

Consider a circular bombing process of intensity λ. For a circle of radius r, the probability p_2 that a point chosen at random on the plane is isolated is equal to the probability that there is no circle within a radius r around the point as its center. Thus $p_2 = \exp(-\pi r^2\lambda) = \exp(-\lambda\alpha)$, where α is the area of a circle. The proportion p_1 of the plane covered by circles is the probability that a point is not isolated:

$p_1 = 1-p_2 = 1-\exp(-\lambda\alpha)$. Notice that if we drop two circles of area $1/2\alpha$ every time we previously dropped a single circle, the area covered will be unchanged. The fact that two small circles cannot possibly combine to produce the same shape as a single larger circle suggests that the area covered is independent of the shape of the dropped figures.

Theorem III: If an infinite collection of congruent convex figures, each of area α, are isotropically, independently, and homogeneously distributed throughout the plane, then the proportion p_1 of the plane covered by the figures is $1-\exp(-\lambda_\alpha)$.

Proof: This follows directly from Theorem I. Let K_o be a point on the plane. The number N of randomly dropped figures K intersecting the point K_o has a Poisson distribution with mean $\lambda\alpha$, where α is the area of K. Therefore

$$f(N) = \frac{1}{N!} (\lambda\alpha)^N e^{-\lambda\alpha}$$

The probability p_2 that a point is isolated is the probability that N=0:

$$p_2 = Pr(N=0) = f(0) = e^{-\lambda\alpha}.$$

The probability p_1 that a point is not isolated is therefore $1-e^{-\lambda\alpha}$.

Theorem III relates the number of dropped figures to the proportion of the plane covered:

$$\lambda = \frac{-1}{\alpha} \ln(1-p_1) = -\frac{1}{\alpha} \ln p_2$$

This is a useful equation for estimating the number of particles on a microscope slide, parts on a conveyor belt, trees in a field, etc.

Examples of bombing processes

a) Random Line Segment Process $L(\tau,\ell)$

Line segments each of length ℓ are distributed isotropically over the plane. The orientation of a line segment is specified by the angle Θ between the x-axis and the perpendicular to the line segment. The midpoint (x_o,y_o) of the line segment specifies its position.

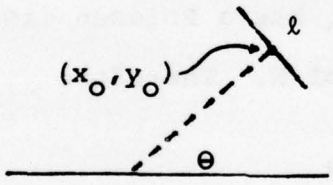

Assume that we are given two line segments centered at randomly selected points P and Q, with an angle Θ between them. They will intersect if P falls within a rhombus of side length ℓ centered at Q.

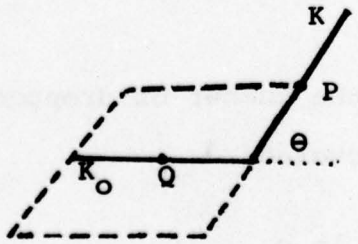

The area of the rhombus is $\ell^2 \sin\theta$, so that we have

$$m(K_o,K) = 2\int_o^{\pi} \tfrac{1}{2}\ell^2 \sin\theta \, dF\theta = 2\int_o^{\pi} \frac{\ell^2}{2\pi} \sin\theta \, d\theta = \frac{2\ell^2}{\pi} .$$

Thus from Theorem I, the number N of randomly distributed line segments of length ℓ intersecting a fixed line segment of length ℓ has a Poisson distribution with mean $\frac{2\lambda\ell^2}{\pi}$:

$$f(N) = \frac{1}{N!} \left(\frac{2\lambda\ell^2}{\pi} \right)^N \exp\left(\frac{-2\lambda\ell^2}{\pi} \right) .$$

The probability p_o that a line segment is isolated is the probability that N is zero.

$$p_o = Pr(N=0) = f(0) = \exp(-2\lambda\ell^2/\pi) .$$

b) Elliptical Bombing Process $E(\lambda, c_1, c_2, \mu_1, \Sigma_1, \mu_2, \Sigma_2)$

Ellipses having major axis $2c_1$ and minor axis $2c_2$ are distributed randomly over the plane. The orientation of an ellipse is specified by the angle θ between the x-axis and the perpendicular to the major axis of the ellipse. The midpoint of the ellipse specifies its position.

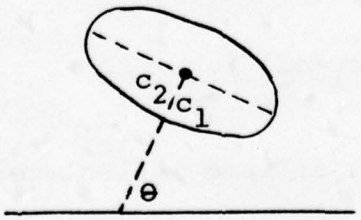

The parametric equations for the ellipse are

$$x - x_o = c_1 \cos\alpha \cos\theta - c_2 \sin\alpha \sin\theta$$

$$y - y_o = c_1 \cos\alpha \sin\theta + c_2 \sin\alpha \cos\theta;$$

where α is between 0 and 2π. Thus

$$\frac{(x-x_o)}{c_1}\cos\theta + \frac{(y-y_o)}{c_1}\sin\theta = \cos\alpha$$

$$-\frac{(x-x_o)}{c_2}\sin\theta + \frac{(y-y_o)}{c_2}\cos\theta = \sin\alpha$$

The equation for the interior of the ellipse is

$$\left\{ \left[\frac{(x-x_o)}{c_1}\cos\theta + \frac{(y-y_o)}{c_1}\sin\theta\right]^2 + \left[-\frac{(x-x_o)}{2_2}\sin\theta + \frac{(y-y_o)}{c_2}\cos\theta\right]^2 < 1 \right\}$$

The area of the ellipse is $\alpha = \pi c_1 c_2$, and the perimeter is

$L = 4c_1 E\left(\sqrt{\frac{c_1^2+c_2^2}{2}}\right) 2\pi$, using elliptical integral tables for E.

From Theorem II, the number N of randomly distributed ellipses intersecting a fixed ellipse has a Poisson distribution with mean

$$2\lambda c_1\left[\pi c_2 + \frac{4c_1 E}{\pi}\right] \approx \pi\lambda[c_1+c_2]^2].$$

The probability that an ellipse is isolated is

$$p_o = \Pr(N=0) = f(0) \approx \exp[-\pi\lambda[c_1+c_2]^2].$$

A realization of an ellipsoidal bombing process is shown in Figure 9a.

c) Circular Bombing Process [12] $C[\lambda, c, \mu_1, \Sigma_1, \mu_2, \Sigma_2)$

A circular bombing process is a special case of the elliptical bombing process, where $c_1 = c_2 = c$ (Fig. 9b).

Any two circles in the plane will overlap if the distance between their centers is less than their diameter. The probability p_o that a circle is isolated is equal to the probability that there is no circle center within radius 2r of a center point placed randomly on the plane. That is, $p_o = e^{-4\pi r^2 \lambda}$.

The transition probabilities for this process are given by Switzer [13]:

$$p_1 P_{11}(d) = (2p_1 - 1) + (1-p_1)^{H(d/r)}$$

where $$H(d/r) = \begin{cases} 1 + \left(\frac{d}{\pi r}\right)\sqrt{1 - \left(\frac{d^2}{4r^2}\right)} + \left(\frac{2}{\pi}\right)\sin^{-1}\left(\frac{d}{2r}\right) & \text{for } d \leq 2r \\ 2 & \text{for } d > 2r \end{cases}$$

$$P_{12}(d) = (p_1/p_2)\, P_{21}(d)$$

$$P_{22}(d) = 1 - P_{12}(d)$$

$$P_{21}(d) = 1 - P_{11}(d)$$

A special case of the circular bombing process occurs when each of the circles covers only one pixel. The process then becomes one of randomly thrown Gaussian noise (Fig. 9c).

d) Rectangular Bombing Process $R(\lambda, c_1, c_2, \mu_1, \Sigma_1, \mu_2, \Sigma_2)$

Rectangles of major axis $2c_1$ and minor axis $2c_2$ are randomly dropped onto the plane. The orientation of a rectangle is specified by the angle Θ between the x axis and the

perpendicular to the major axis of the rectangle. The midpoint of a rectangle specifies its position.

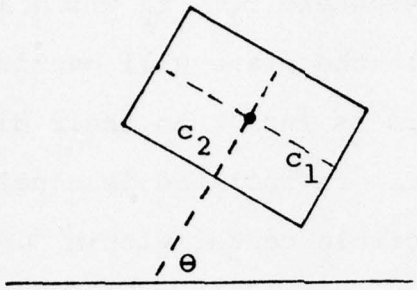

A realization of a rectangular bombing process is shown in Fig. 9d.

The equationsfor a rectangle are

$$|(x-x_o)\cos\theta + (y-y_o)\sin\theta| = c_1$$

$$|-(x-x_o)\sin\theta + (y-y_o)\cos\theta| = c_2$$

The interior of the rectangle is specified by

$$\{\left|\frac{(x-x_o)}{c_1}\cos\theta + \frac{(y-y_o)}{c_1}\sin\theta\right| < 1;\ \left|-\frac{(x-x_o)}{c_2}\sin\theta + \frac{(y-y_o)}{c_2}\cos\theta\right| < 1\}$$

From Theorem II, the number N of randomly distributed rectangles intersecting a fixed rectangle has a Poisson distribution with mean $8\lambda(c_1c_2 + \frac{1}{\pi}(c_1+c_2)^2)$. The probability that a rectangle is isolated is:

$$p_o = Pr(N=0) = f(0) = \exp(-8\lambda(c_1c_2 + \tfrac{1}{\pi}(c_1+c_2)^2)).$$

Rectangles of one pixel thickness can be used to approximate Poisson line segments (Fig. 9f).

5. Statistics

The statistical properties of our models can be obtained directly from the stationary and transition probabilities. Note that we have given transition probabilities only for three models -- Poisson Line, Checkerboard, and Circular Bombing. We will assume that each region A_i is colored by a Gaussian random vector process having parameters μ_i and Σ_{ii}. Let

$$f(x,\mu_i,\Sigma_{ii}) = \frac{1}{(2\pi)^{q/2}|\Sigma|^{\frac{1}{2}}} \exp\left[-\frac{1}{2}(x-\mu)^t\Sigma^{-1}(x-\mu)\right]$$

a) Histogram

Let H(c) denote the probability that a point on an image has color c, where c is a q-element vector. For example, for visual color

$$H(c) = \Pr\begin{bmatrix}\text{red content of point } s = c_1\\ \text{green content of point } s = c_2\\ \text{blue content of point } s = c_3\end{bmatrix}.$$

Then

$$H(c) = \sum_{i=1}^{m} p_i f(c,\mu_i,\Sigma_{ii})$$

b) Cooccurrence

Drop a Buffon needle of length d onto a picture. The endpoints of the needle are denoted by s and s'. $\Pr\binom{c_k}{c_\ell}$ denotes the probability that s lands on color c_k and s' lands on color c_ℓ. Then

$$\Pr\binom{c_k}{c_\ell} = \sum_{j=1}^{m} \sum_{i=j}^{m} \Pr(s\varepsilon A_i, s'\varepsilon A_j)\ \Pr[\text{color}(s) = c_k \text{ and color}(s') = c_\ell \mid s\varepsilon A_i, s'\varepsilon A_j]$$

where $\Pr(s\varepsilon A_i, s'\varepsilon A_j) = p_j P_{ij}(d)$, and

$$\Pr[\text{color}(s)=c_k,\ \text{color}(s')=c_\ell \mid s\varepsilon A_i, s'\varepsilon A_j] = f[\binom{c_k}{c_\ell},\ \binom{\mu_i}{\mu_j},\ \sum(d)]$$

$$\sum(d) = \begin{bmatrix} \Sigma_{ii}(0) & \Sigma_{ij}(d) \\ \Sigma_{ji}(d) & \Sigma_{jj}(0) \end{bmatrix}$$

If there is no correlation across region boundaries, we have

$$\Pr\binom{c_k}{c_\ell} = \sum\sum_{i\neq j} \Pr(s\varepsilon A_i, s'\varepsilon A_j) \Pr[\text{color}(s)=c_k,\ \text{color}(s')=c_\ell \mid s\varepsilon A_i, s'\varepsilon A_j]$$

$$+ \sum_i P_r(s, s'\varepsilon A_i)\ \Pr[\text{color}(s)=c_k,\ \text{color}(s')=c_\ell \mid s, s'\varepsilon A_i]$$

$$= \sum_{i\neq j} P_j P_{ij}(d)\ f[\binom{c_k}{c_\ell},\ \binom{\mu_i}{\mu_j},\ \hat{\sum}(d)]$$

$$+ \sum_i P_i\ P_{ii}(d)\ f[\binom{c_k}{c_\ell},\ \binom{\mu_i}{\mu_i},\ \sum(d)]$$

where

$$\hat{\sum}(d) = \begin{bmatrix} \Sigma_{ii}(0) & 0 \\ 0 & \Sigma_{jj}(0) \end{bmatrix}$$

In the cell structure models discussed in Section 3, where it is assumed that cells are independently colored, we have no correlation across cell boundaries, and we obtain

$$P_r\begin{pmatrix} c_k \\ c_\ell \end{pmatrix} = \sum_{i \neq j} P_j P_{ij}(d)\ f\left[\begin{pmatrix} c_k \\ c_\ell \end{pmatrix}, \begin{pmatrix} \mu_i \\ \mu_j \end{pmatrix}, \hat{\Sigma}(d)\right]$$

$$+ \sum_i P_i^2 (1-W(d))\ f\left[\begin{pmatrix} c_k \\ c_\ell \end{pmatrix}, \begin{pmatrix} \mu_i \\ \mu_i \end{pmatrix}, \hat{\Sigma}(d)\right]$$

$$+ \sum_i P_i W(d)\ f\left[\begin{pmatrix} c_k \\ c_\ell \end{pmatrix}, \begin{pmatrix} \mu_i \\ \mu_i \end{pmatrix}, \Sigma(d)\right]$$

(3) Difference

Again drop a needle of length d onto a picture. Let $\mathcal{D}(\Delta)$ denote the sum over all colors c of the probability that s' lands on color c+Δ and s lands on color c. Then

$$\mathcal{D}(\Delta) = \sum_i \sum_j \int_c P_r(s \varepsilon A_i, s' \varepsilon A_j) P_r[\text{color}(s) = c,\ \text{color}(s') = c+\Delta \mid s \varepsilon A_i, s' \varepsilon A)]$$

The equations under various assumptions are analogous to those for cooccurrence.

(6) Variogram

Again drop a needle of length d onto a picture. Let V(d) denote the mean squared color difference at the endpoints of the needle. Then

$$V(d) = E[(\text{color}(s)-\text{color}(s'))^t\ (\text{color}(s)-\text{color}(s'))]$$

If there is no correlation across region boundaries we get

$$V(d) = \sum_i \sum_j [\Sigma_{ii}(d) + \Sigma_{jj}(d) + (\mu_i-\mu_j)^t\ (\mu_i-\mu_j)] P_j P_{ij}(d)$$

For the cell structure models, there is no correlation across cell boundaries, and we have

$$V(d) = \sum_{i \neq j} \sum_{j} [\Sigma_{ii}(0) + \Sigma_{jj}(0) + (\mu_i - \mu_j)^t (\mu_i - \mu_j)] P_j P_{ij}(d)$$

$$+ \sum_{i} [2\Sigma_{ii}(d)] P_i W(d)$$

$$+ \sum_{i} [2\Sigma_{ii}(0)] P_i^2 [1 - W(d)] .$$

6. Discussion

We have presented a number of models for random spatial pattern. They not only provide interesting descriptions of pattern formation processes, but also suggest the following projects for future research.

Given a pattern, we might attempt to determine the best fitting model. Hopefully, this will offer some insight into the pattern's structure and even into the type of natural process that created it. Preliminary work in this direction was done in an earlier report [19]. If we can derive the parameters of a model from a pattern, then we can neatly characterize the pattern as a realization of a particular random process.

We have given the sets of parameters required by each of our models. These parameters could be used as features to discriminate between different models or different realizations of the same model. Texture discrimination problems are fundamental to the automated analysis of remote sensing data and medical imagery.

Our models could also be used to generate textures. Current computer generated imagery represents textured surfaces by white noise or repeated patterns. Random textures will add realism to computer animated films. Realistic computer generated images can also be used for visual perception experiments. These will offer other insights into texture perception than those obtained through the use of random dot patterns.

Much of the research on these models was done by statistical ecologists -- Matern, Pielou, and Switzer. They were interested in reconstructing planar maps from coarsely sampled data. They compared estimated maps constructed by different sampling schemes, under different source errors. These same techniques could be used to reconstruct a coarsely sampled image.

In an attempt to better understand these models, parameters that cannot be determined analytically might be obtained by a Monte Carlo simulation. For example, Crain and Miles [21] generated 200,000 Poisson line polygons to estimate some important unknown distribution properties of cell vertices, perimeter, and area. A similar study could be undertaken to obtain the transition probabilities and cell statistics of the occupancy and Johnson-Mehl models.

A number of other models for random spatial pattern are available. A broader study is needed to compare and catalog them. Mandlebrot [14] models irregular and fragmentary natural patterns by Brownian surfaces (Fig. 10). Wong [16], Hassner [17], and others model images by two-dimensional random fields. Matheron [18] and a number of other French mathematicians describe random spatial patterns in terms of regionalized random variables. Further study of such models in connection with texture analysis and synthesis would be desirable.

Figure 1. A realization of a two-dimensional Poisson point process with $\lambda = 50$.

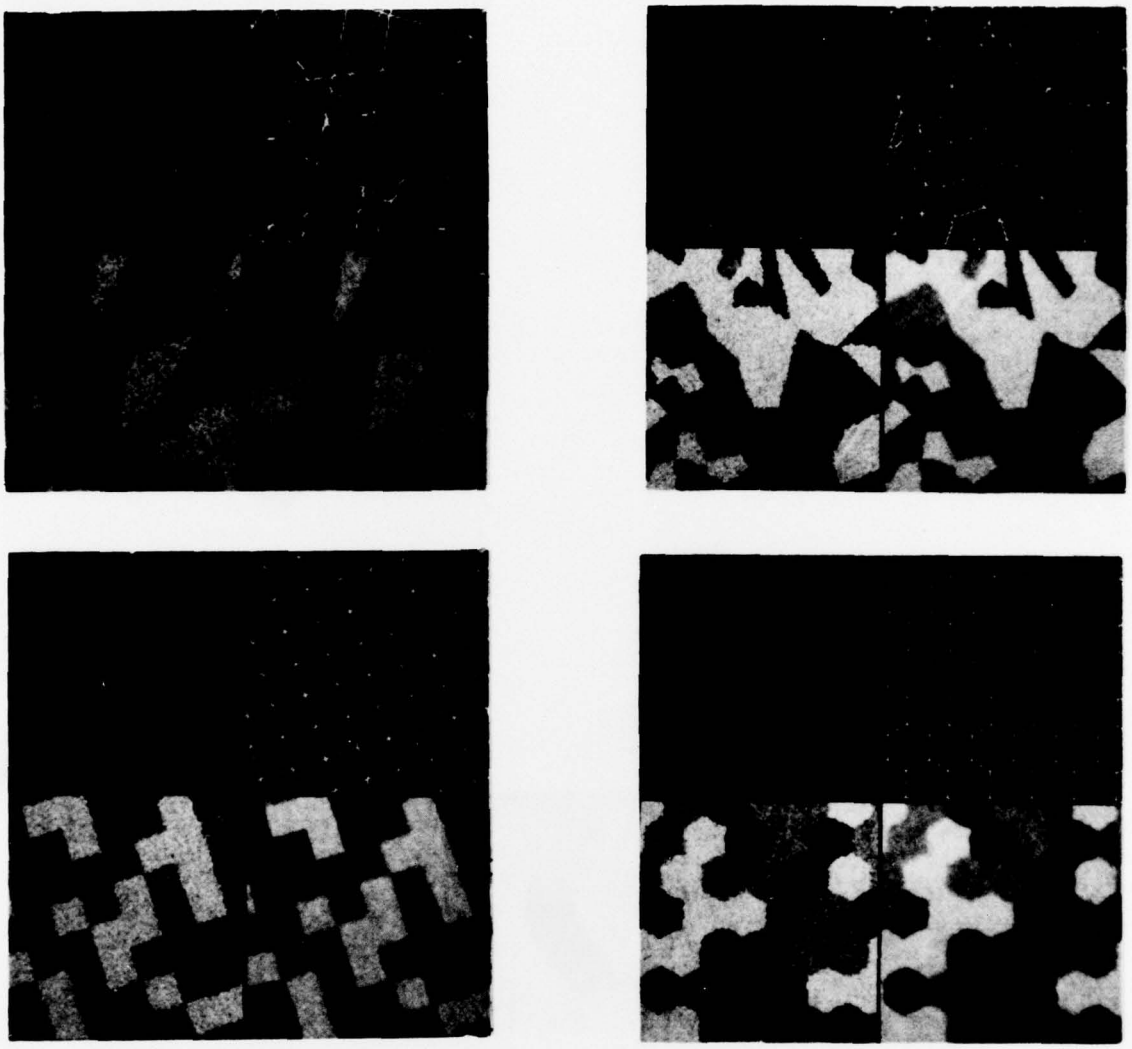

Figure 2. Cell structure models.

a) Poisson line tessellation
b) $L(16,(.33,.33,.34),(15,30,45),(25,25,25))$
c) 2b mean filtered over a 3-by-3 neighborhood
d) Occupancy model tessellation
e) $O(40,(.33,.33,.34),(15,30,45),(25,25,25))$
f) 2e mean filtered over a 3-by-3 neighborhood
g) Rotated checkerboard tessellation
h) $C(\frac{10}{127},(.33,.33,.34),(15,30,50),(25,25,25))$
i) 2h mean filtered over a 3-by-3 neighborhood
j) Rotated hexagonal tessellation
k) $H(40,(.33,.33,.34),(15,30,45),(25,25,25))$
l) 2.k mean filtered over a 3-by-3 neighborhood

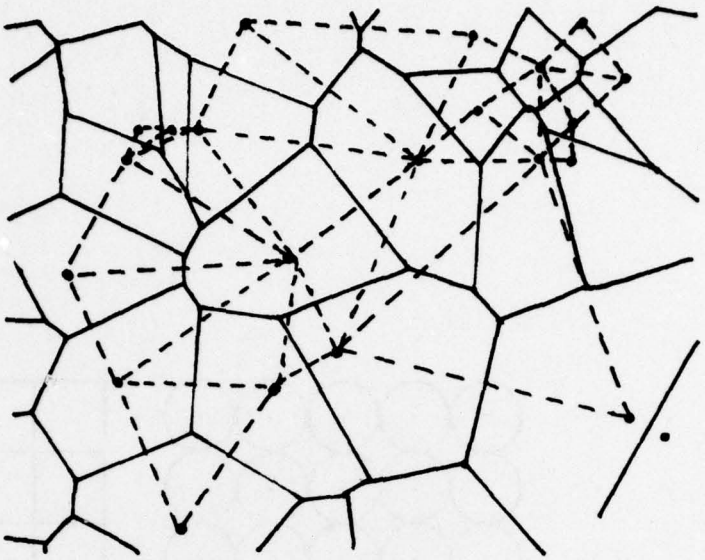

Figure 3. Cells generated by occupancy model. Delaunay triangles shown as dashed lines.

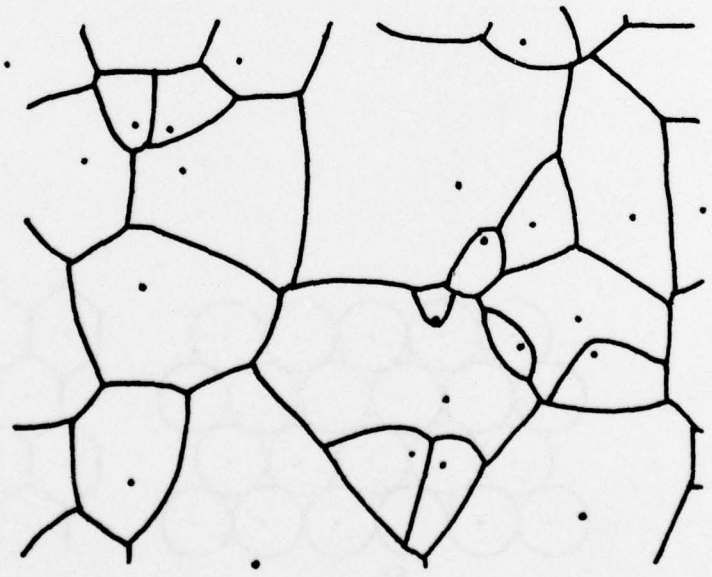

Figure 4. Cells generated by the Johnson-Mehl model. (From [7].)

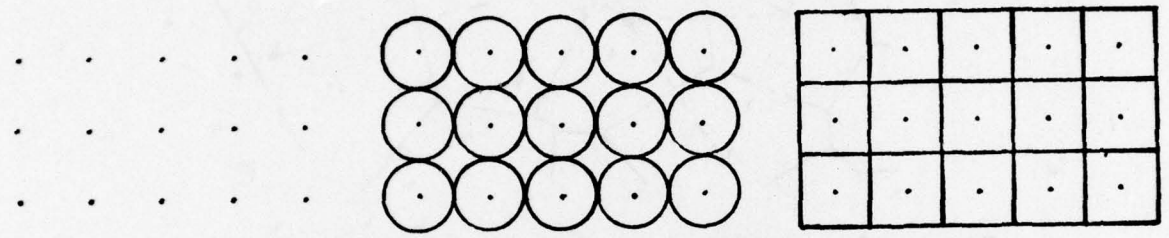

Figure 5. Square growth process.

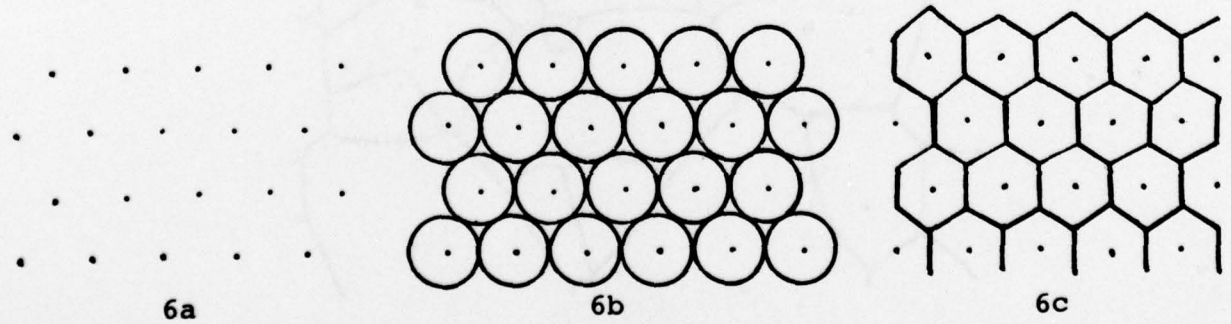

Figure 6. Hexagonal growth process.

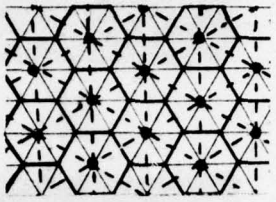

Figure 7. Hexagonal tessellation.

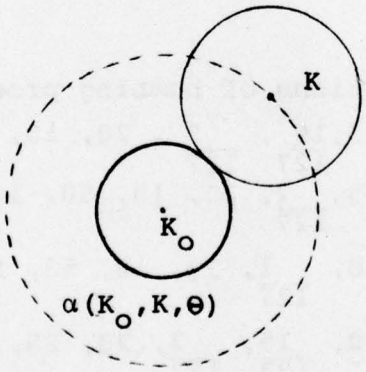

Figure 8. $\alpha(K_o, K, \Theta)$ for two circles.

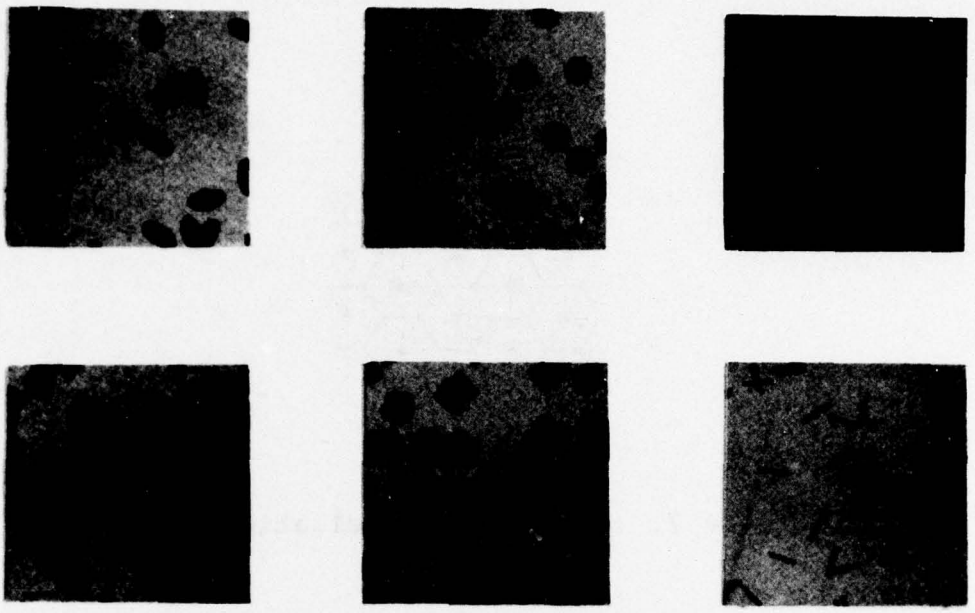

Figure 9. Realizations of bombing processes.

a) $E(25, \frac{10}{127}, \frac{5}{127}, 20, 10, 50, 10)$

b) $C(25, \frac{7}{127}, 20, 10, 50, 10)$

c) $C(40, \frac{1}{127}, 13, 10, 53, 10)$

d) $R(30, \frac{15}{127}, \frac{7}{127}, 20, 25, 40, 25)$

e) $S(30, \frac{7}{127}, 20, 10, 50, 10)$

f) $R(30, \frac{10}{127}, \frac{1}{127}, 20, 10, 50, 10)$

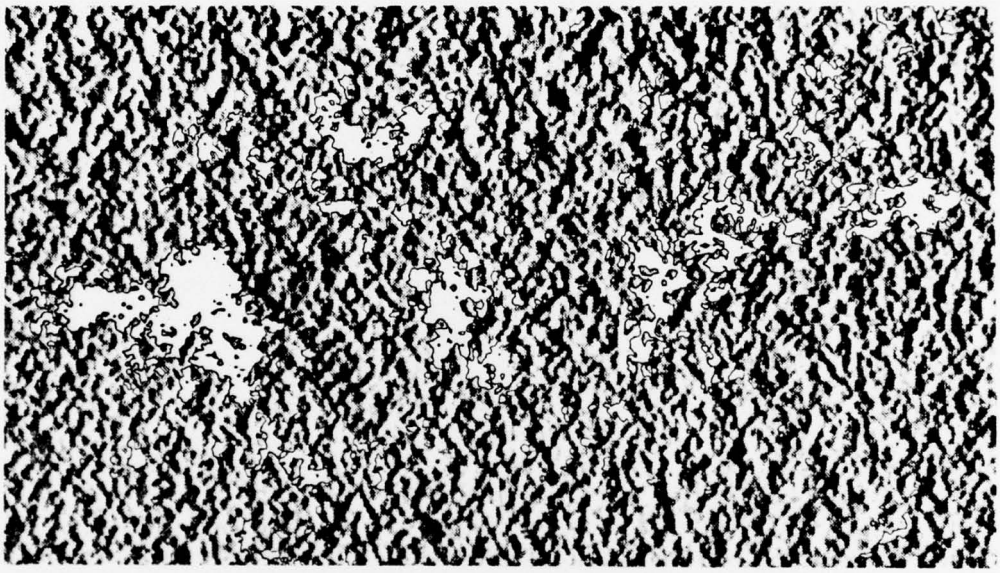

Figure 10. Brownian surface texture.
(From [14].)

References

1. M. S. Bartlett, The Statistical Analysis of Spatial Pattern, John Wiley, NY, 1975.

2. B. Matern, Doubly Stochastic Poisson Processes in the Plane, Statistical Ecology 1, U. of Penn. Press, 1971, 195-213.

3. R. B. Root, Some Consequences of Ecosystem Texture, Ecosystem Analysis and Prediction, Soc. Ind. Appl. Math., Philadelphia, 1975, 83-97.

4. E. Pielou, An Introduction to Mathematical Ecology, Wiley, NY, 1969.

5. P. Switzer, A Random Set Process In the Plane With a Markovian Property, Ann. Math. Stat. 36, 1965, 1859-1863.

6. M. Shamos and D. Hoey, Closest-Point Problems, 16th Annual IEEE Symposium on Foundations of Computer Science, 1975, 151-162.

7. E. Gilbert, Random Subdivisions of Space Into Crystals, Ann. Math. Stat. 33, 1962, 958-972.

8. R. Miles, On the Homogeneous Planar Poisson Point-Process, Math. Biosciences 6, 1970, 85-127.

9. B. Matern, Spatial Variation, Medd Statens Skogsforsknings-institut,Stockholm, 36(5), 1-144, 1960.

10. D. Thompson, On Growth and Form (Vol. II), Cambridge, University Press, 1963.

11. D. Dufour, Intersections of Random Convex Regions, Stanford University, Dept. of Statistics, T.R. 202, 1973.

12. S. Roach, The Theory of Random Clumping, Methuen and Co., Ltd., London, 1968.

13. P. Switzer, Reconstructing Patterns From Sample Data, Annals Math. Stat. 38, 1967, 138-154.

14. B. Mandelbrot, Fractals - Form, Chance, and Dimension, Freeman, San Francisco, 1977.

15. S. Zucker, Toward a Model of Texture, Computer Graphics and Image Processing 5, 1976, 190-202.

16. E. Wong, Two-Dimensional Random Fields and Representations of Images, SIAM J. Appl. Math. 16(4), 1968, 756-770.

17. M. Hassner, Markov Models of Digitized Images - A Data Compression Analysis, Submitted to IEEE Trans. on Information Theory.

18. G. Matheron, The Theory of Regionalized Variables And Its Applications, Les Cahiers du Centre de Morphologie Math. de Fontainbleau 5, 1971.

19. B. Schachter, A. Rosenfeld, and L. Davis, Random Mosaic Models for Textures, University of Maryland Computer Science T.R. 463, July 1976.

20. M. Puzin, Simulation of Cellular Patterns by Computer Graphics, University of Toronto Dept. of Computer Science T.R. 10, May 1969.

21. I. Crain and R. Miles, Monte Carlo Estimates of the Distribution of the Random Polygons Determined by Random Lines in a Plane, J. Statistical Computer Simulation 4, 1976, 293-325.

UNCLASSIFIED

SECURITY CLASSIFICATION OF THIS PAGE (When Data Entered)

REPORT DOCUMENTATION PAGE		READ INSTRUCTIONS BEFORE COMPLETING FORM
1. REPORT NUMBER AFOSR-TR- 77 - 1225	2. GOVT ACCESSION NO.	3. RECIPIENT'S CATALOG NUMBER
4. TITLE (and Subtitle) A SURVEY OF RANDOM PATTERN GENERATION PROCESSES		5. TYPE OF REPORT & PERIOD COVERED 6. PERFORMING ORG. REPORT NUMBER TR-549
7. AUTHOR(s) Bruce Schachter and Narendra Ahuja		8. CONTRACT OR GRANT NUMBER(s) AFOSR-77-3271
9. PERFORMING ORGANIZATION NAME AND ADDRESS Computer Science Ctr. U. of Maryland College Pk., MD 20742		10. PROGRAM ELEMENT, PROJECT, TASK AREA & WORK UNIT NUMBERS 61102F 2304/A2
11. CONTROLLING OFFICE NAME AND ADDRESS Math.& Info. Sciences, AFOSR/NM Bolling AFB Wash., DC 20332		12. REPORT DATE July 1977 13. NUMBER OF PAGES
14. MONITORING AGENCY NAME & ADDRESS(if different from Controlling Office)		15. SECURITY CLASS. (of this report) UNCLASSIFIED 15a. DECLASSIFICATION/DOWNGRADING SCHEDULE

16. DISTRIBUTION STATEMENT (of this Report)

Approved for public release; distribution unlimited.

17. DISTRIBUTION STATEMENT (of the abstract entered in Block 20, if different from Report)

18. SUPPLEMENTARY NOTES

19. KEY WORDS (Continue on reverse side if necessary and identify by block number)

Pattern recognition
Image processing
Random geometry
Texture

20. ABSTRACT (Continue on reverse side if necessary and identify by block number) Random pattern generation processes can provide a rich class of models for both the synthesis and analysis of visual textures. This report describes a variety of such processes including point processes, random mosaic processes, and bombing processes. Standard texture analysis approaches (e.g., cooccurrence matrices) are related to texture models based on these random processes. Examples of several textures synthesized by computer in accordance with these models are presented.

DD FORM 1 JAN 73 1473 EDITION OF 1 NOV 65 IS OBSOLETE

UNCLASSIFIED

SECURITY CLASSIFICATION OF THIS PAGE (When Data Entered)